PNAS
www.pnas.org

Supplementary Information for

Nanchung and inactive define pore properties of the native auditory transduction channel in *Drosophila*

Bingxue Li[a,b,1], Songling Li[a,b,1], Honglan Zheng[a,b], Zhiqiang Yan[a,b,2]

[a]State Key Laboratory of Medical Neurobiology and MOE Frontiers Center for Brain Science, Institute of Brain Science, School of Life Sciences, Fudan University, Shanghai 200438, China.

[b]Institute of Molecular Physiology, Shenzhen Bay Laboratory, Shenzhen 518132, China.

[1]These authors contributed equally to this work.

[2]Correspondence to: Zhiqiang Yan
Email: *zqyan@szbl.ac.cn*

This PDF file includes:

Figures S1 to S18
SI References

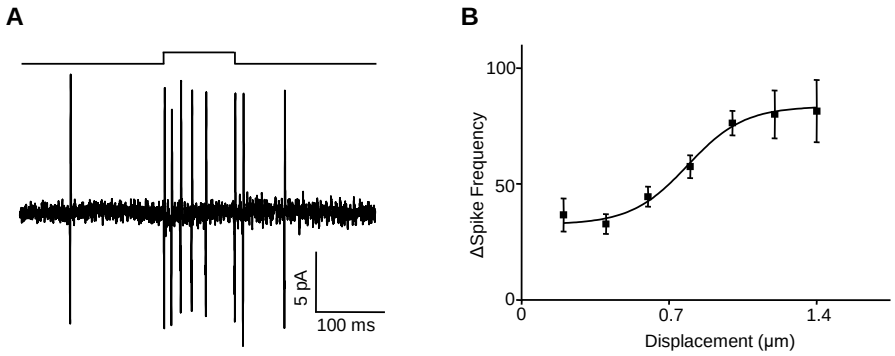

Fig. S1. Lch1 neurons respond to mechanical stimuli with action potential firings. (*A*) Touching the dendrite tip of a lch1 neuron with a 1 μm displacement induced a burst of action potentials. (*B*) Summary of action potential firings of lch1 neurons in response to progressively greater mechanical stimuli. ΔSpike Frequency: increase in the frequency of action potentials after stimulus onset compared to 100 ms before stimulus onset (n = 6, 11, 11, 8, 8, 6, 7). The displacements were from 0.2 μm to 1.4 μm with 0.2 μm increments. Error bars, mean ± SEM.

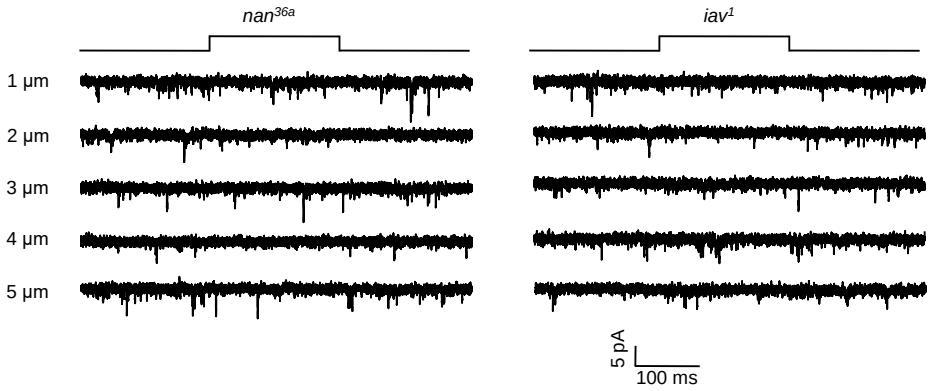

Fig. S2. No mechanical stimuli-induced currents are detected in lch1 neurons of *nan* and *iav* mutants in response to increasing stimuli. Lch1 neurons were held at -60 mV. *nan*^{36a}, *Nanchung* null mutant; *iav*^{1}, *Inactive* null mutant. 1 µm, 2 µm, 3 µm, 4 µm, and 5 µm represent the displacements of mechanical stimuli. Genotypes are as follows: for *iav*^{1}: *iav*^{1}/y; Iav-Gal4/+; UAS-CD8-GFP/+. For *nan*^{36a}: Iav-Gal4/UAS-GFP; *nan*^{36a}/ *nan*^{36a}.

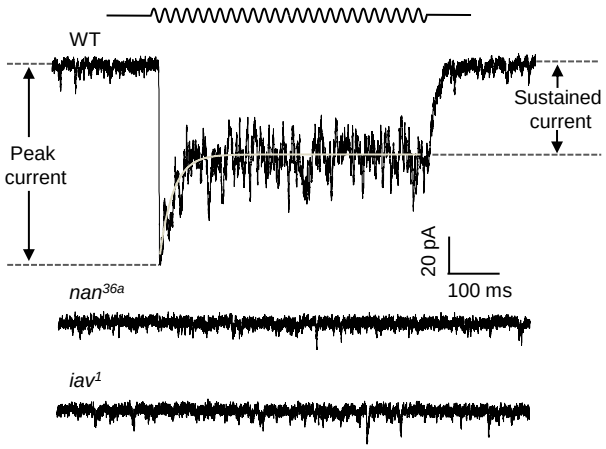

Fig. S3. Sound-induced currents in Cho neurons. Representative traces of current responses to a 500Hz 90 dB pure tone sound stimulation in wild-type and *nan*^{36a}, *iav*^{1} mutants. Lch1 neurons were held at -60 mV. The sound-elicited transduction current is similar to those recorded from locust auditory receptor neurons in a previous study (1). The grey line overlying the trace represents a single exponential fit of adaptation of the sound-induced current.

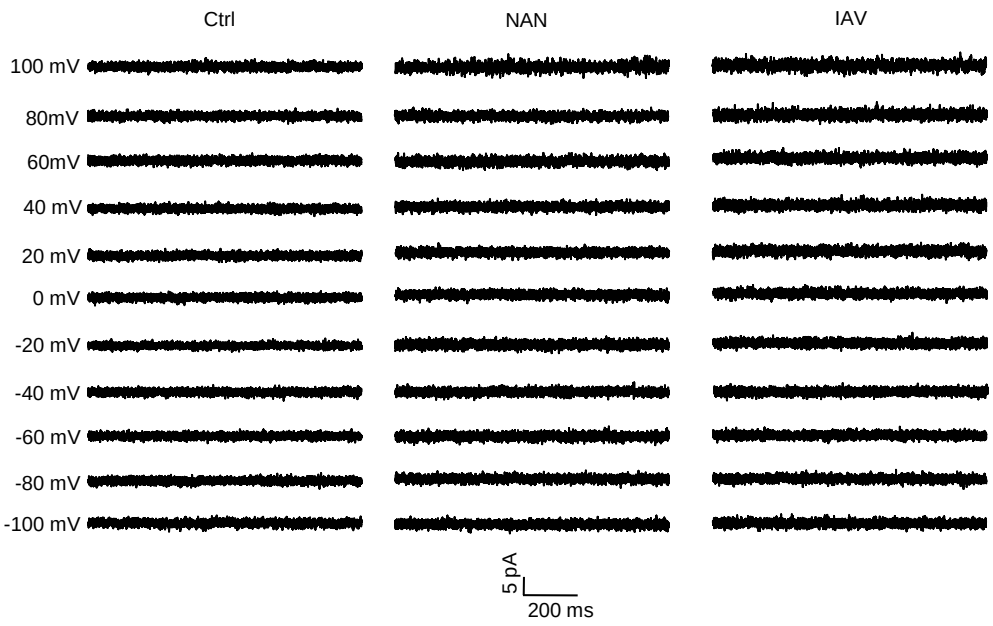

Fig. S4. Representative traces of single channel activities in control, NAN and IAV transfected S2 cells. S2 cells were clamped at potentials ranging from -100 to +100 mV (holding potentials) with 20 mV increments and recorded with a K^+-based internal solution and a Na^+-based extracellular solution. Ctrl, nontransfected S2 cells; NAN, S2 cells transfected with NAN-Flag; IAV, S2 cells transfected with IAV-mCherry.

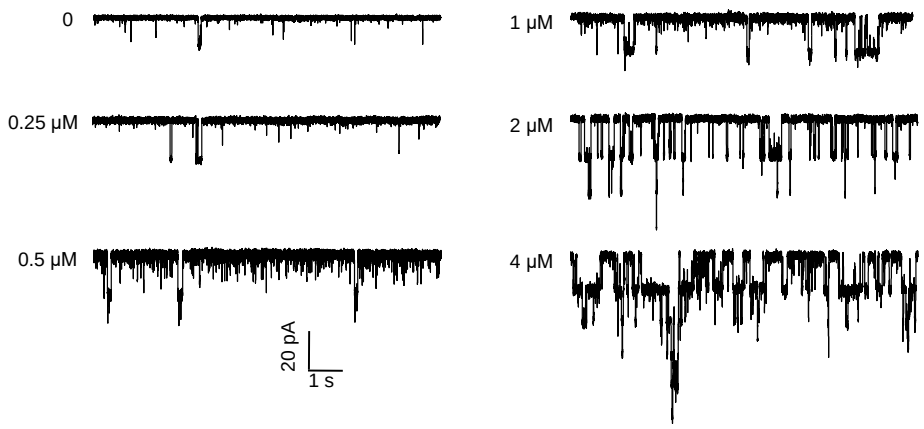

Fig. S5. Representative traces of single channel activities in Inactive-mCherry- and Nanchung-Flag-coexpressing S2 cells with or without NAM. The concentrations of nicotinamide (NAM) in the K^+-based pipette solution during the whole-cell recordings were 0, 0.25 μM, 0. 5 μM, 1 μM, 2 μM, and 4 μM. The holding potential was -60 mV.

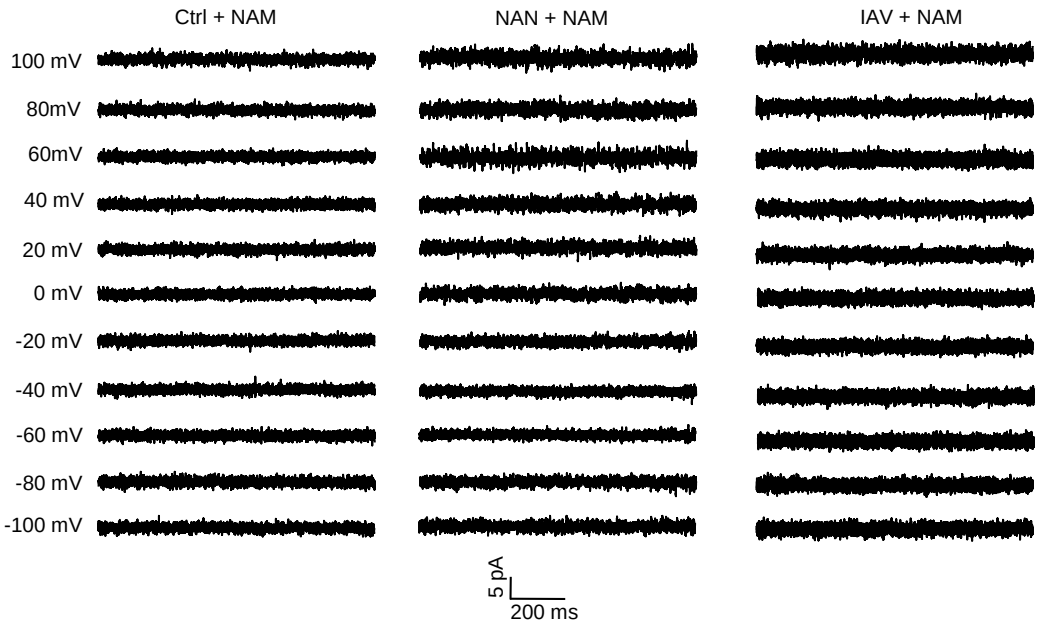

Fig. S6. Representative traces of single channel activities in empty, NAN and IAV transfected S2 cells with NAM. S2 cells were clamped at potentials ranging from -100 to +100 mV (holding potential). Ctrl+NAM, nontransfected S2 cells; NAN+NAM, S2 cells transfected with NAN-Flag; IAV+NAM, S2 cells transfected with IAV-mCherry. All the K^+-based pipette solutions contained 2 μM NAM.

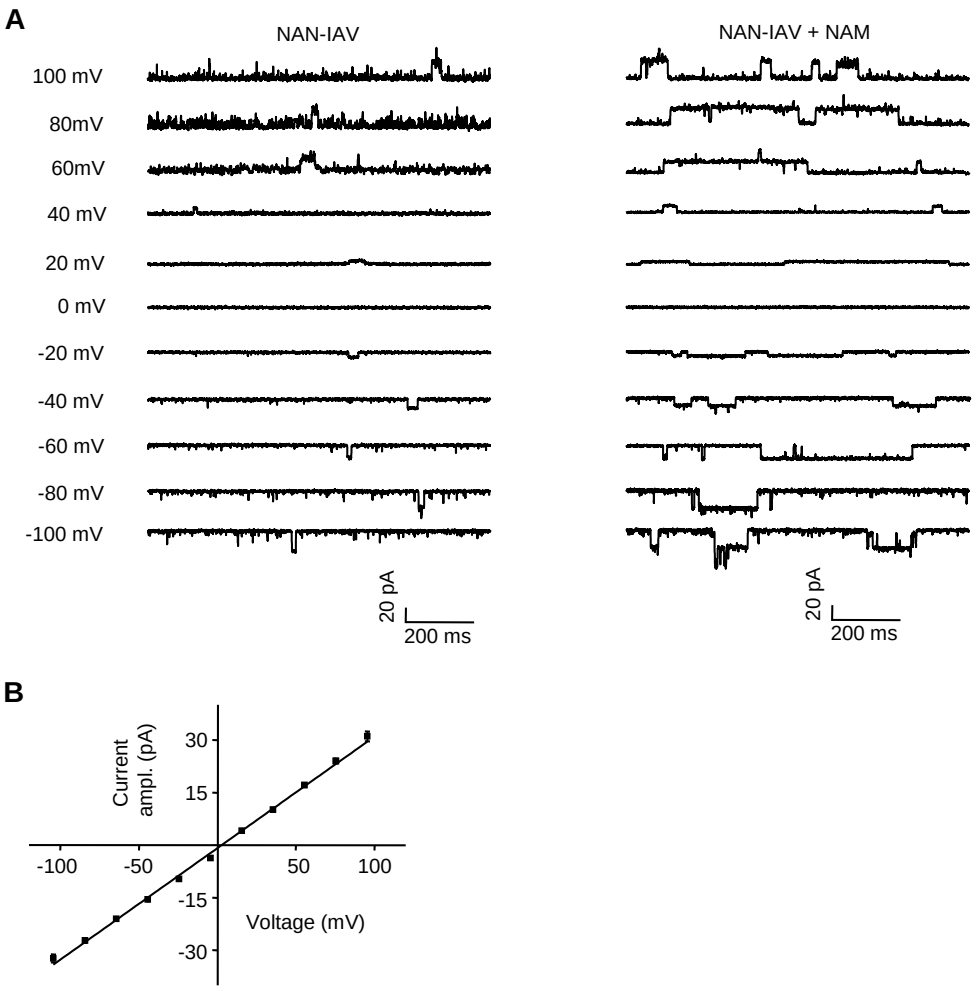

Fig. S7. NAN-IAV single channel activities with voltage steps in S2 cells. (*A*) Single channel current traces of NAN-IAV with voltage steps in the extracellular Na^+/ intracellular K^+ condition. NAN-IAV, spontaneous single channel activity in normal Na^+/K^+ solution; NAN-IAV+NAM, active single channel current with 2 μM NAM in internal solution. Cells were clamped at potentials ranging from -100 to +100 mV (holding potential). (*B*) I-V curves of NAN-IAV single channel currents in Na^+/K^+ conditions with 2 μM NAM in pipette solution (n = 5). Error bars, mean ± SEM. The liquid junction potential was +4.5 mV; the holding potentials were from -100 mV to +100 mV; the membrane potentials (X axis) were from -104.5 mV to +95.5 mV with 20 mV increments.

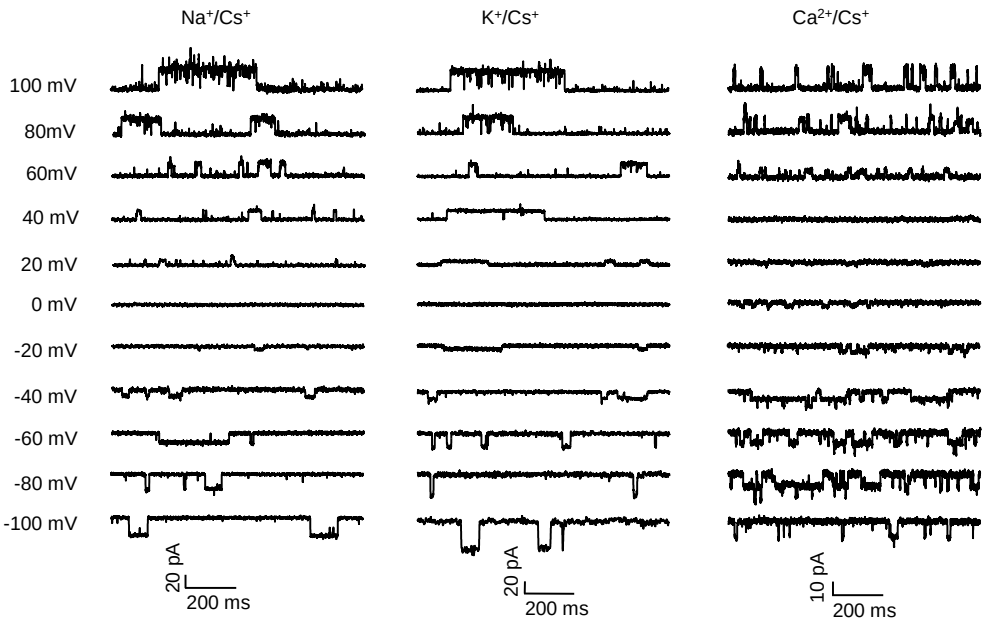

Fig. S8. Single channel current traces of NAN-IAV with voltage steps in bi-ionic conditions in S2 cells. S2 cells were clamped at potentials ranging from -100 to +100 mV (holding potentials). Na^+/Cs^+, extracellular Na^+/intracellular Cs^+; K^+/Cs^+, extracellular K^+/intracellular Cs^+; Ca^{2+}/Cs^+, extracellular Ca^{2+}/intracellular Cs^+. All the internal solutions contained 2 μM NAM.

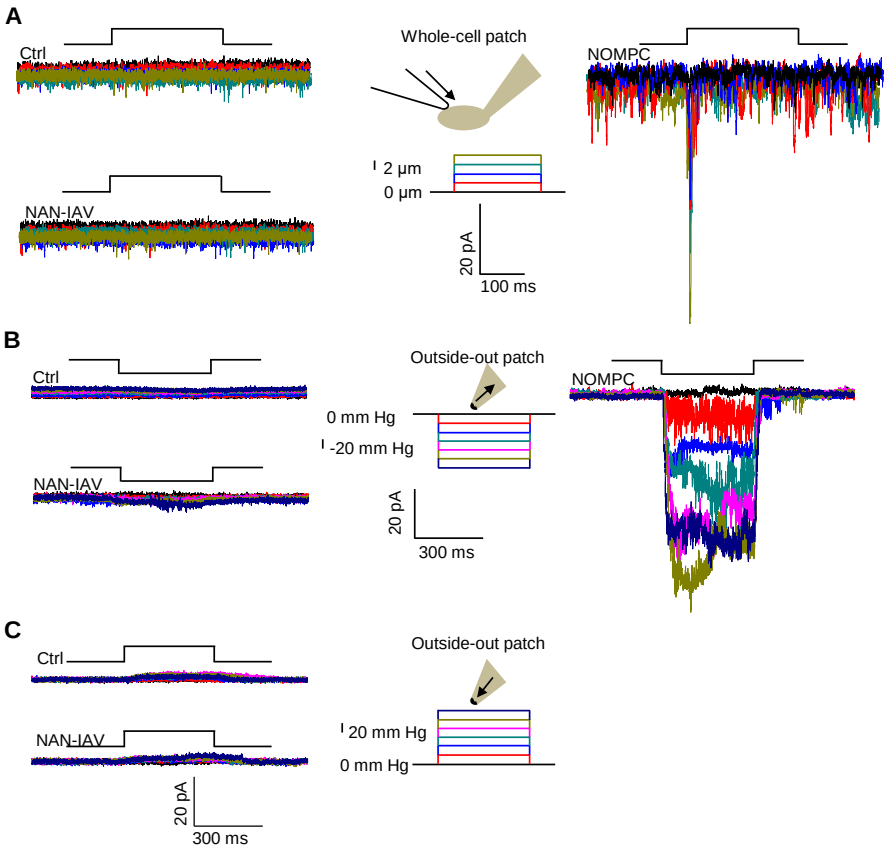

Fig. S9. Electrophysiological recordings of NAN-IAV or NOMPC in S2 cells. (*A*) Representative traces of control, NAN-IAV or NOMPC transfected S2 cells for whole-cell patch recordings in response to 2-8 µm mechanical displacements. The black arrow denotes the direction of mechanical displacements. The holding potential is -60 mV. (*B*) Representative traces of control, NAN-IAV or NOMPC transfected S2 cells for outside-out patch recordings in response to -20– -120 mmHg negative pressure. The black arrow denotes negative pressure. The holding potential is -60 mV. (*C*) Representative traces of control, NAN-IAV or NOMPC transfected S2 cells for outside-out patch recordings in response to +20– +120 mmHg positive pressure. The black arrow denotes negative pressure. The holding potential is -60 mV.

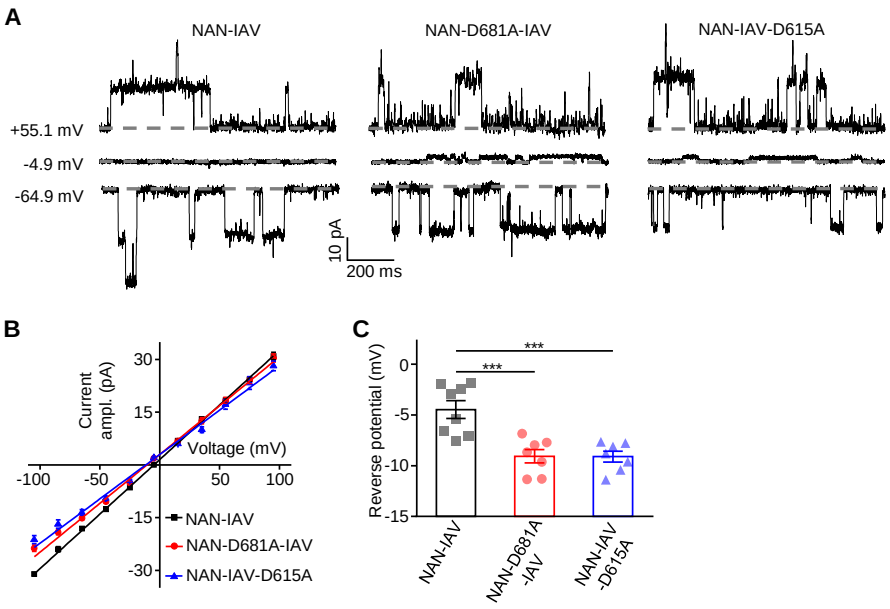

Fig. S10. Point mutations of NAN and IAV in selective filter region altered the reversal potential of NAN-IAV channels in S2 cells. (*A*) Representative traces of single channel activities in wild-type and mutant NAN-IAV channels at -60 mV (holding potential) in Na^+/Cs^+-based solutions with 2 μM nicotinamide (NAM) in internal solution. Gray dashed lines denote the closed states of single channel. The liquid junction potential is +4.9 mV; the holding potentials are -60 mV, 0 mV, +60 mV; the membrane potentials are -64.9 mV, -4.9 mV, +55.1 mV. (*B*) Average current-voltage relationship of wild-type and mutant NAN-IAV single channel currents in Na^+/Cs^+-based solutions with NAM (n = 8, 7, 7; mean ± SEM). The liquid junction potential is +4.9 mV; the holding potentials are from -100 mV to +100 mV; the membrane potentials (X axis) are from -104.9 mV to +95.1 mV with 20 mV increments. NAND681A-IAV, S2 cells transfected with NAN-D681A-Flag and IAV-mCherry; NAN-IAV-D615A, S2 cells transfected with NAN-Flag and IAV-D615A-mCherry. (*C*) Summary of reversal potentials of single channel currents of wild-type and point mutant NAN-IAV in S2 cells (n = 8, 7, 7; mean ± SEM). One-way analysis of variance followed by Holm–Sidak post hoc analysis was used for comparison among multiple groups. ***p < 0.001.

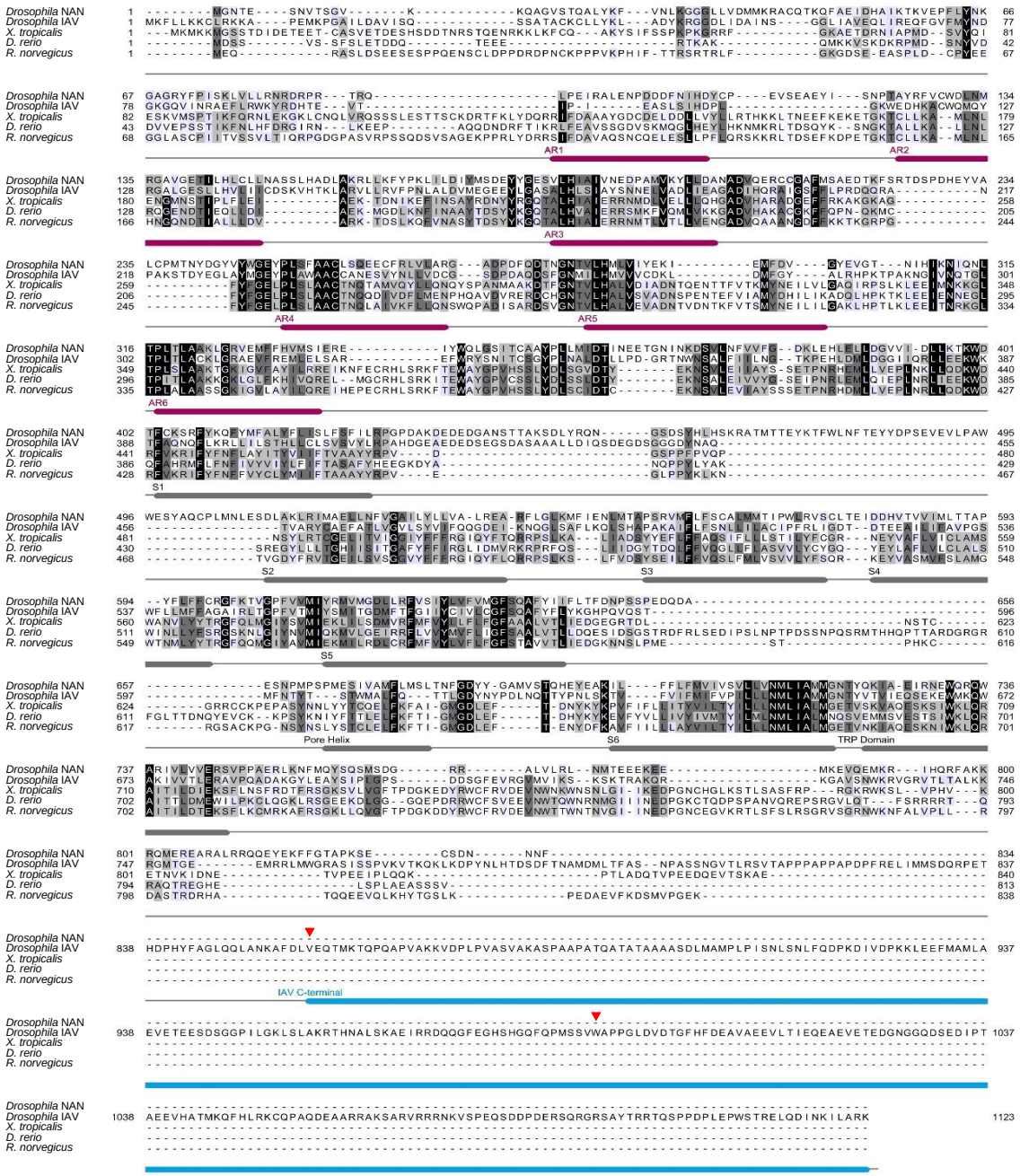

Fig. S11. Sequence alignment of TRPV Orthologues. The sequence homology of *Drosophila* IAV and NAN to other TRPV1 orthologs was analyzed by Clustal Omega. Secondary structure elements and the C-terminal region of IAV are indicated below the sequence. Red arrowheads mark the two residues 857 and 990.

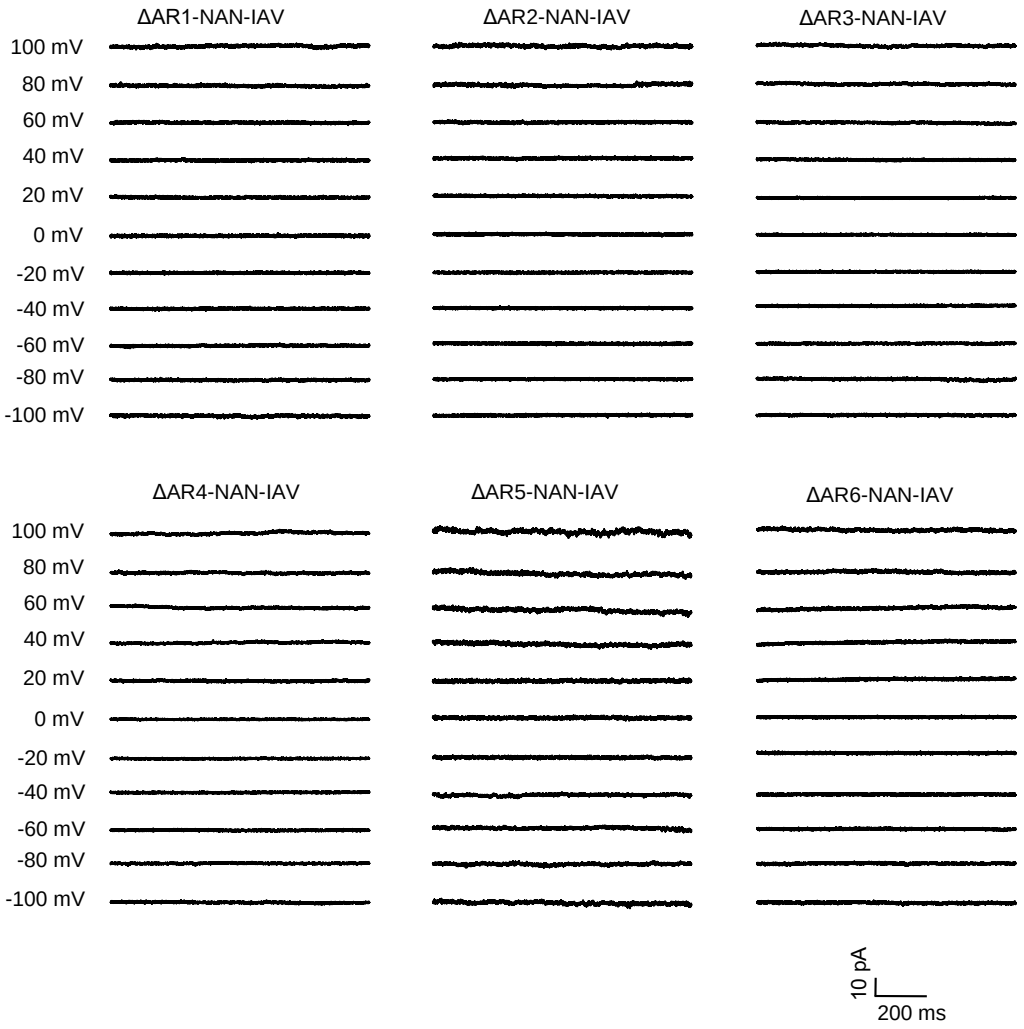

Fig. S12. Representative traces of single channel activities in truncated NAN transfected S2 cells. S2 cells were recorded at holding potentials ranging from -100 to +100 mV with 20 mV increments in Na^+/K^+-based solutions. ΔAR, deletion of ankyrin repeats; ΔAR1-NAN-IAV, S2 cells transfected with ΔAR1-NAN-Flag and IAV-mCherry; ΔAR2-NAN-IAV, S2 cells transfected with ΔAR2-NAN-Flag and IAV-mCherry; ΔAR3-NAN-IAV, S2 cells transfected with ΔAR3-NAN-Flag and IAV-mCherry; ΔAR4-NAN-IAV, S2 cells transfected with ΔAR4-NAN-Flag and IAV-mCherry; ΔAR5-NAN-IAV, S2 cells transfected with ΔAR5-NAN-Flag and IAV-mCherry; ΔAR6-NAN-IAV, S2 cells transfected with ΔAR6-Cherry. All the pipette solutions contained 2 μM NAM.

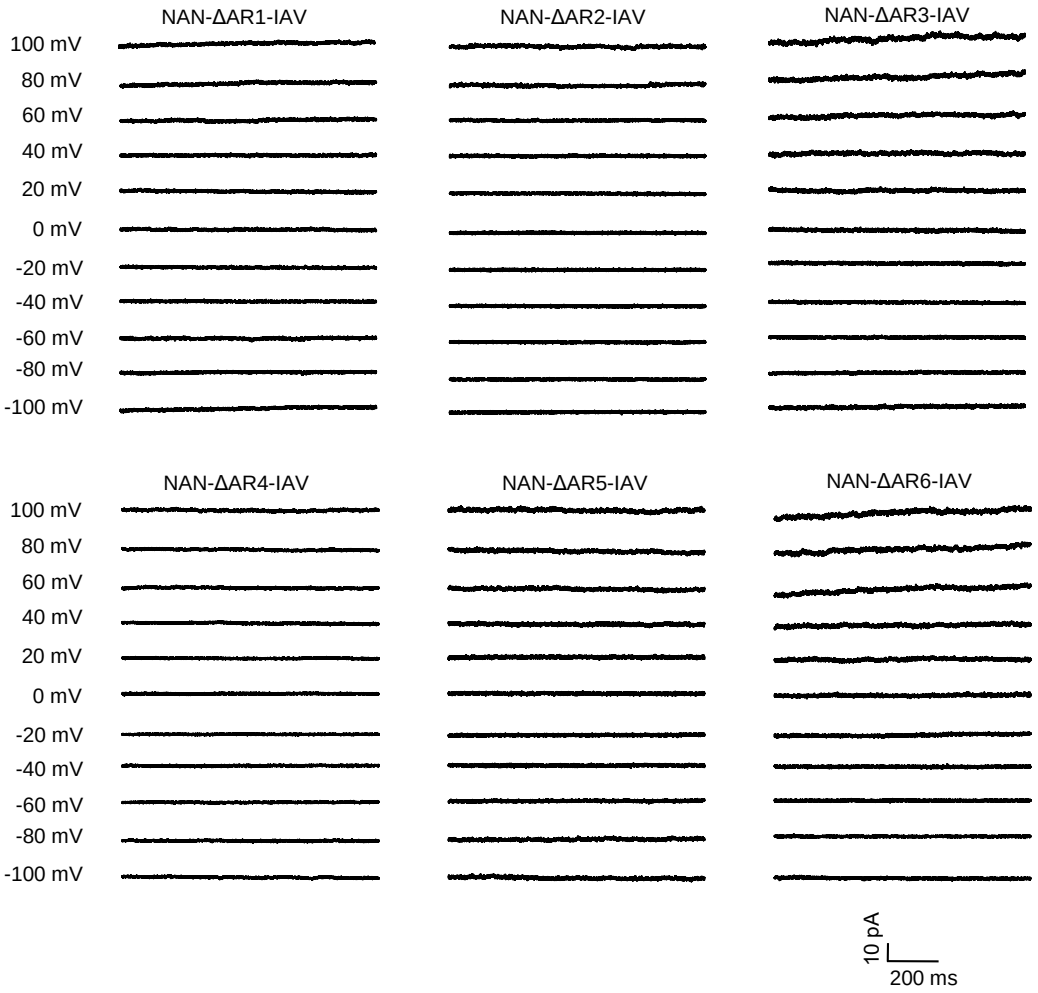

Fig. S13. Representative traces of single channel activities in truncated IAV transfected S2 cells. S2 cells were clamped at holding potentials ranging from -100 to +100 mV. ΔAR, deletion of Ankyrin repeats; NAN-ΔAR1-IAV, S2 cells transfected with NAN-Flag and ΔAR1-IAV-mCherry; NAN-ΔAR2-IAV, S2 cells transfected with NAN-Flag and IAV-ΔAR2-mCherry; NAN-ΔAR3-IAV, S2 cells transfected with NAN-Flag and IAV-ΔAR3-mCherry; NAN-ΔAR4-IAV, S2 cells transfected with NAN-Flag and IAV-ΔAR4-mCherry; NAN-ΔAR5-IAV, S2 cells transfected with NAN-Flag and IAV-ΔAR5-mCherry; NAN-ΔAR6-IAV, S2 cells transfected with NAN-Flag and IAV-ΔAR6-mCherry. All of the K^+-based pipette solutions contained 2 μM NAM.

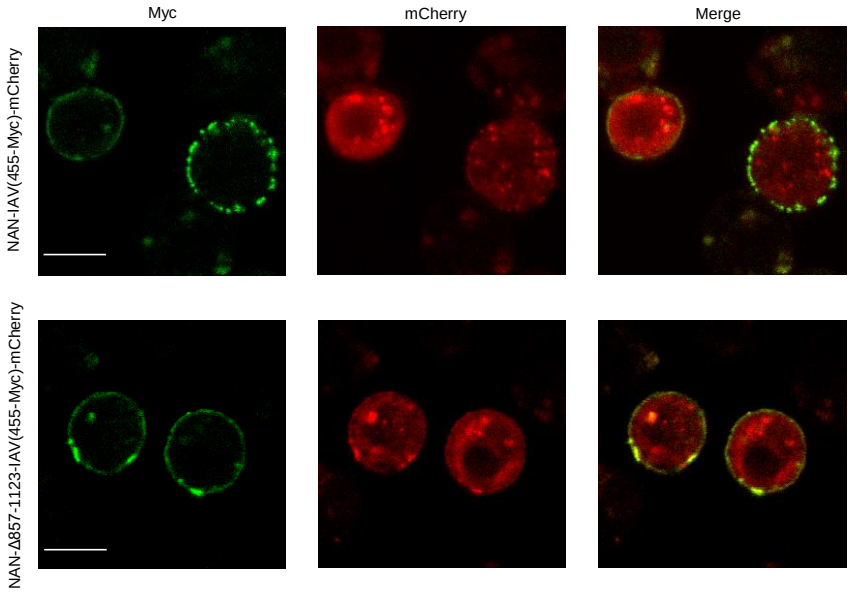

Fig. S14. Immunostaining of S2 cells expressing NAN-IAV and NAN-Δ857-1123-IAV. Representative images of myc staining in NAN-IAV-mCherry- and NAN-Δ857-1123-IAV-mCherry-transfected S2 cells. Myc tags were inserted behind the Q455 residue of IAV. Scale bar, 10 μm.

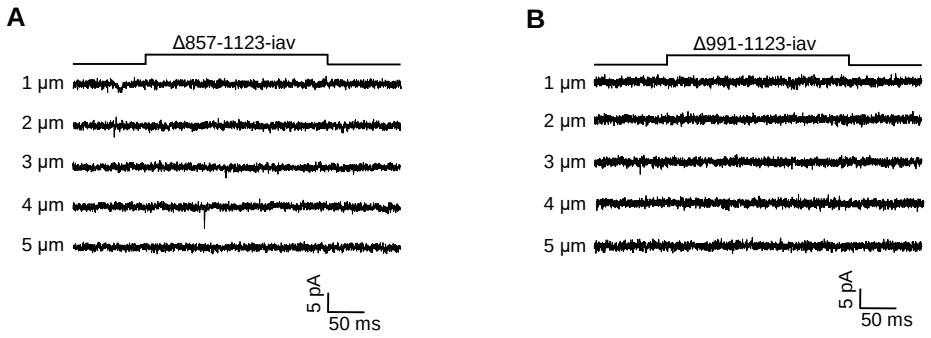

Fig. S15. No MET currents were detected in lch1 neurons of two truncated mutants of *iav* in response to increasing stimuli. (*A*, *B*) Δ857-1123-iav and Δ991-1123-iav could not rescue the MET currents of *iav*^{1}. Lch1 neurons were clamped at -60 mV (holding potential) in Na^{+}/K^{+}-based solutions. Values of 1 μm, 2 μm, 3 μm, 4 μm, and 5 μm represent the displacements of mechanical stimuli. Genotypes are as follows: for *A*, Δ857-1123-iav: *iav*^{1}/y; Iav-Gal4/+; UAS-Δ857-1123-iav-GFP/+. For *B*, Δ991-1123-iav: *iav*^{1}/y; Iav-Gal4/+; UAS-Δ991-1123-iav-GFP/+.

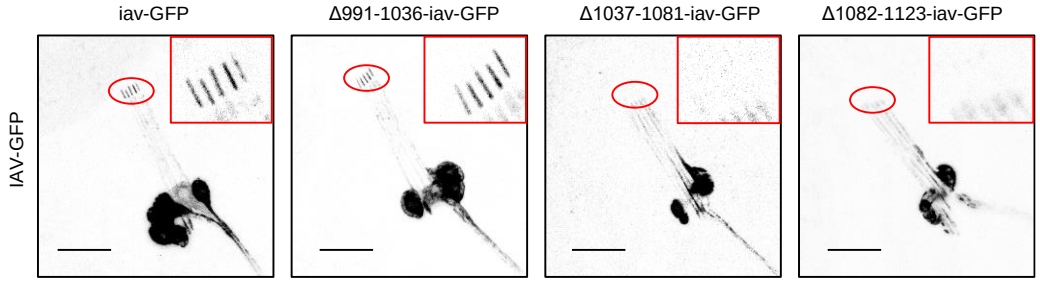

Fig. S16. Localization of wild-type and mutant forms of IAV in lch5 neurons of *iav*^{1} mutant larvae. Expression of GFP-tagged constructs were driven by Iav-Gal4 driver. Scale bar, 20 μm. Genotypes are as follows: iav-GFP: *iav*^{1}/y; Iav-Gal4/+; UAS-iav-GFP/+. Δ991-1036-iav-GFP: *iav*^{1}/y; Iav-Gal4/+; UAS-Δ991-1036-iav-GFP/+. Δ1037-1081-iav-GFP: *iav*^{1}/y; Iav-Gal4/+; UAS-Δ1037-1081-iav-GFP/+. Δ1082-1123-iav-GFP: *iav*^{1}/y; Iav-Gal4/+; UAS-Δ1082-1123-iav-GFP/+.

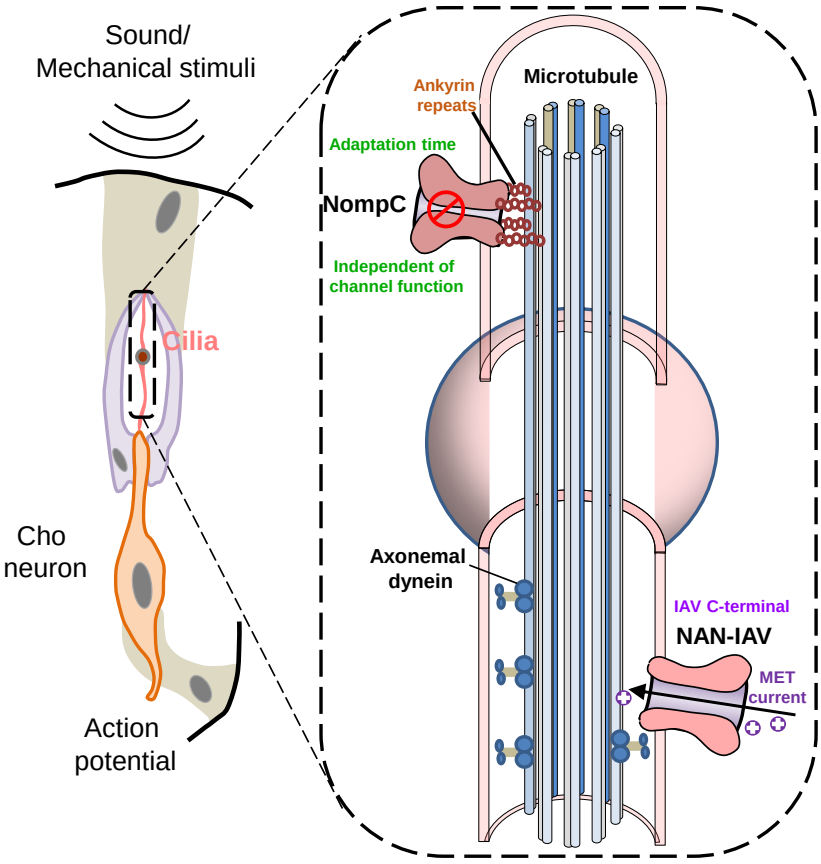

Fig. S17. A schematic of auditory transduction in *Drosophila* larval Cho neurons. At the tip of the dendrite, each Cho neuron bears a cilium (Left), which displays an axoneme containing microtubular doublets and dynein arm-like protrusions (Right). Nanchung and Inactive are localized to the proximal cilia, while NompC has a restricted distribution in the distal cilia (Right).

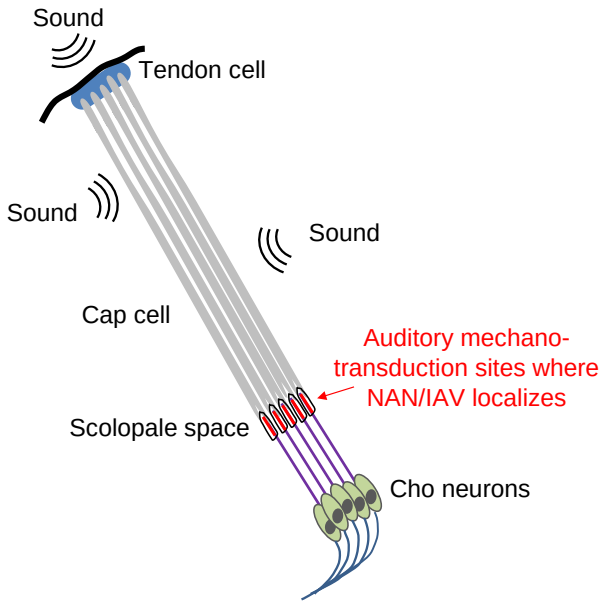

Fig. S18. The scolopidia structure of *Drosophila* auditory organs. The illustration of chordotonal organs was adapted from a previous study (2). Adapted by permission from Springer Nature Customer Service Centre GmbH: Springer Nature, Neuroscience Bulletin; Axonemal Dynein DNAH5 is Required for Sound Sensation in Drosophila Larvae. Li B, Li S, Yan Z, © 2021. The cilia of Cho neurons, where auditory transduction take place, are surrounded with scolopale space, and the ciliary tips project into cap cells, which are attached to the cuticles through tendon cells.

SI References

1. B. Warren, T. Matheson, The Role of the Mechanotransduction Ion Channel Candidate Nanchung-Inactive in Auditory Transduction in an Insect Ear. *J. Neurosci.* **38**, 3741-3752 (2018).
2. B. Li, S. Li, Z. Yan, Axonemal Dynein DNAH5 is Required for Sound Sensation in Drosophila Larvae. *Neurosci. Bull.* **37**, 523-534 (2021).